Materials Science & Engineering A 701 (2017) 237–244

Contents lists available at ScienceDirect

Materials Science & Engineering A

journal homepage: www.elsevier.com/locate/msea

Liquid phase sintering of mechanically alloyed Mo-Cu powders

Paola A. Benavides[a,*], Benjamín Soto[b], Rodrigo H. Palma[b]

[a] Doctoral program in Engineering Sciences, mention Science of the Materials, University of Chile, Santiago, Chile, Universidad Tecnológica de Chile INACAP, Santiago, Chile

[b] Department of Mechanical Engineering, University of Chile. Santiago, Chile

ARTICLE INFO

Keywords:
Mo-Cu alloy
Mechanical alloying
Liquid phase sintering
Microstructure
Hardness
SEM

ABSTRACT

In the Mo-Cu system, Mo has very low solubility in liquid Cu. To reach high densities after liquid phase sintering it is required the solution-reprecipitation step, which induces shape change. One technique that allows to form solids solutions out of equilibrium is the mechanical alloying. In the present work, the effect of the mechanical alloying of the elemental Mo and Cu (10, 20 and 30 vol%) powders and the sintering atmosphere (Ar vs Ar + 10 vol% H_2) on the densification, microstructure and hardness of sintered samples in liquid phase at 1150 °C for 1 h, was studied. It is hypothesized that the sintering can be facilitated by the generation of a solid solution of Mo in Cu out of equilibrium which, allows the Mo to enter solution in the Cu liquid and re-precipitate on the solid Mo particles during the process.

The results show that mechanically alloyed Mo-Cu and sintered powders in the reducing atmosphere of Ar + 10 vol% H_2, have the highest densities and densification of all studied alloys. This is explained by the formation of solid solution of Mo in Cu during the mechanical alloying, evidenced by the EDS analysis. It is suggested that these milled and sintered powders reach the highest hardness due to their microstructural refinement, high density of Mo dislocations and low porosity.

1. Introduction

Mo-Cu alloys have been investigated for many years because of their relatively low and constant coefficient of thermal expansion (of up to 1073 K) and their high thermal and electrical conductivity, which make them suitable for contact materials in cooling and electronic packages [1]. The significant difference between the melting points of both metals and their insolubility make traditional metallurgical processes inappropriate to obtain these alloys due to their the high-energy consumption. The infiltration method by which a pre-sintered porous Mo skeleton infiltrates with Cu, high density obtained, but this method is a complex process due to Cu exudation and grain growth in the microstructure [2]. Liquid phase sintering (LPS) of mixed microcrystalline powders usually does not reach high density since the solution-reprecipitation (SR) step requires solid constitutes (Mo) to enter in liquid phase (Cu) leading to the change of shape and thus increasing density will not occur. Due the mutual insolubility of the solid and liquid state of Mo and Cu [3–5].

The Mechanical Alloying (MA) is a method developed over the past decades (since the 1970s), which allows an increase in the solubility of the insoluble elemental powders outside of the equilibrium [2,5,6]. In this method, the powders are subjected to repetitive impacts at high speed, which cause plastic deformation and hardening and cold welding. At the same time, together with the hardening, the fracture of the powders occurs. All the processes are continuously repeated to achieve the desired results of mechanical alloying [6,7].

The use of the MA method to incorporate Mo in Cu has been studied by Martínez et. al. [7]. It showed an increase of Mo in solid solution in the Cu with the milling time of up to 100 h. The increase in the solubility of Mo in Cu was explained by a thermodynamic analysis. At 21 h, crystallite sizes of approximately 15–40 nm were obtained whereas higher molybdenum powders showed a lower decrease of grain size. After 21 h of grinding, recrystallization and agglomeration processes were observed.

In another work [8], the mechanical alloying of Cu-Mo under a controlled atmosphere of Ar was carried out. The evolution of grain size as a function of milling time was studied and it was determined that, for 50 h of milling time, a minimum crystallite size of 20 nm was reached for the compound powders of Cu-8 at% in Mo.

Xi and others [9] analyzed the AM of binary and ternary systems based on the Cu-Mo alloys. They found the possibility of dissolving Mo up to 10 wt% in copper by MA.

Jinglian and others [10] were able to obtain pre-alloyed Mo-18, 30, and 40 wt% Cu using the sol-spray-drying process in which Mo and Cu

* Corresponding author.
E-mail address: pbenavides@inacap.cl (P.A. Benavides).

http://dx.doi.org/10.1016/j.msea.2017.06.090
Received 29 December 2016; Received in revised form 21 June 2017; Accepted 23 June 2017
Available online 24 June 2017

Table 1
Description of the samples and their characteristics.

Samples	Process Conditions	Sintering atmosphere
Simple mix: (Mo + Cu)m	Elemental powder Mo and Cu mixed Mo − 10 vol%Cu Mo − 20 vol%Cu Mo − 30 vol%Cu	Ar + 10 vol% H_2
MA powders	Elemental powder Mo and Cu Mo − 10 vol%Cu Mo − 20 vol%Cu Mo − 30 vol%Cu	Ar + 10 vol% H_2
Mix: Mo + (Mo + Cu)m-Ar	MA powders + Mo elemental mixed (Mo + (Simple mix) 10 vol%Cu) (Mo + (Simple mix) 20 vol%Cu) (Mo + (Simple mix) 30 vol%Cu)	Ar
Mix: Mo + (Mo + Cu)m-(Ar + 10 vol%H_2)	MA powders + Mo elementary mixed (Mo + (Simple mix) 10 vol%Cu) (Mo + (Simple mix) 20 vol%Cu) (Mo + (Simple mix) 30 vol%Cu)	Ar + 10 vol% H_2.

salts were heated and reduced to a size of 30 nm and 28 nm for the Mo and Cu, respectively. The powders were compacted and sintered in the liquid phase with a controlled atmosphere of H_2. After sintering, high densities (99%) were obtained in the samples with 30 wt% Cu. It was also found that a maximum amount of liquid phase was achieved for 30 wt% Cu; for higher amounts of Cu, the density decreased. This phenomenon was attributed to the high temperature and the volatilization of the copper rich phase.

Song et al. [11] studied the effect of liquid phase sintering of pre-alloyed Mo-15 wt% Cu powders, which were made through the chemical gelling-reduction process. Powders having sizes in the ranges from 100 to 200 nm were obtained. These powders were subjected to three sintering temperatures (1050, 1100, and 1150 °C) under a controlled atmosphere of H_2, reaching a final relative density of 99.59% for the sample sintered at 1150 °C.

Based on the literature review, it can be concluded that to achieve high density of Mo-Cu alloys in the LPS, it is necessary to produce nanometric powders of Mo and Cu using chemical methods. It should be noted that the LPS of mechanically alloyed Mo-Cu powders was not investigated.

In the present study, it is proposed that the SR mechanism can be proceed in three stages to overcome the mutual insolubility of Mo and Cu that prevents the occurrence of SR. In the first stage, during MA occurs the incorporation of Mo in solid solution in the Cu, out of equilibrium. In the second stage, during the LPS and when the Cu-rich phase is transformed from solid to liquid, the Mo atoms of this phase entered into the liquid solution of Cu. In the final stage, the atoms of Mo in the liquid phase would re-precipitate on the particles of solid Mo, leading to the change of form and them, densification. The stages mentioned could occur, since milled powder of Mo must contain Cu in solid solution beyond equilibrium, is a situation similar to what happens in transient liquid phases, in which one of the initial components, the low melting point (Cu in this case) melts and homogenizes the composition until it reaches equilibrium. Then, in this case, liquid Cu would initially be formed in greater quantity than the equilibrium and the amount of liquid would be reduced by homogenization, reaching equilibrium.

During this process, the influence of the mechanical alloying on the density, microstructure, and hardness for elemental Mo-Cu powders was analyzed. Also, the influence of adding Mo elemental powders to the mechanically alloyed Mo-Cu powders was investigated with the aim of increasing the green density of the compact and allowing a higher sintering density to be obtained as compared to the process with only mechanically alloyed powders, which have the difficulties that requires high pressures for compaction to achieve high green density.

Finally, the effect of the atmosphere on densification was investigated by comparing Ar to Ar + 10 vol% H_2. It was expected that H_2 would act to reduce surface oxides of Mo and Cu powders and thus would facilitate the LPS [5].

2. Materials and methods

2.1. Powders

Cu elemental powders with a purity of 99.99% and 90% and the size less than 45 μm of dendritic morphology were purchased from ACU Powder International. Mo powders with 99.95% purity and an average size of 5.1 μm were supplied by Molymet S.A. (Chile).

2.2. Mechanical alloying

(1-x)%Mo-xCu (x = 10, 20 and 30 vol%) powders were milled using a home-made Szegvari Attritor Grinding Mill with 1500 cc capacity stainless steel container at 500 rpm under a controlled atmosphere of Ar with a flow of 1 l/min and Hexane as the controlling agent. The mass ratio of 4.8 mm stainless steel balls to the powder was 10:1. The milling times were 10, 20 and 30 h for each of Mo-Cu alloys. Once the process was completed, the recovered powders were dried for one hour under halogen lamp, and compacted at 450 MPa to fabricate 1.5 g bars with 12 mm diameter which were sintered at 1150 °C for 1 h in a mixture of Ar + 10 vol% H_2 or only Ar and cooled down in the furnace.

Table 1 shows the process conditions for the four series of manufactured alloys and their designation.

2.3. Materials characterization

The elemental powders of Mo and Cu were characterized by scanning electron microscopy (SEM; JEOL, JSM-IT300) and EDS to determine their shape, distribution, size and composition. Structural characteristics of samples were analyzed through X-Ray Diffraction (XRD; Bruker D8), using Cu° Kα1 radiation (λ = 1.5405 Å) with an increase of 0.02° and a passage time of 56.7 s. The sweep angle range varies from 2° < 2θ < 80°. The green density of the samples was obtained by geometrical method. After sintering, the Archimedes Method was used to obtain the density. Porosity was measured from the density by the following Eq. (1):

$$\varepsilon = 1 - \frac{\rho_{final}}{\rho_{theoric}} \quad (1)$$

where ε is the porosity and ρ is the density.

The microstructural features such as type and distribution of present phases were characterized by optical microscope. The Vickers

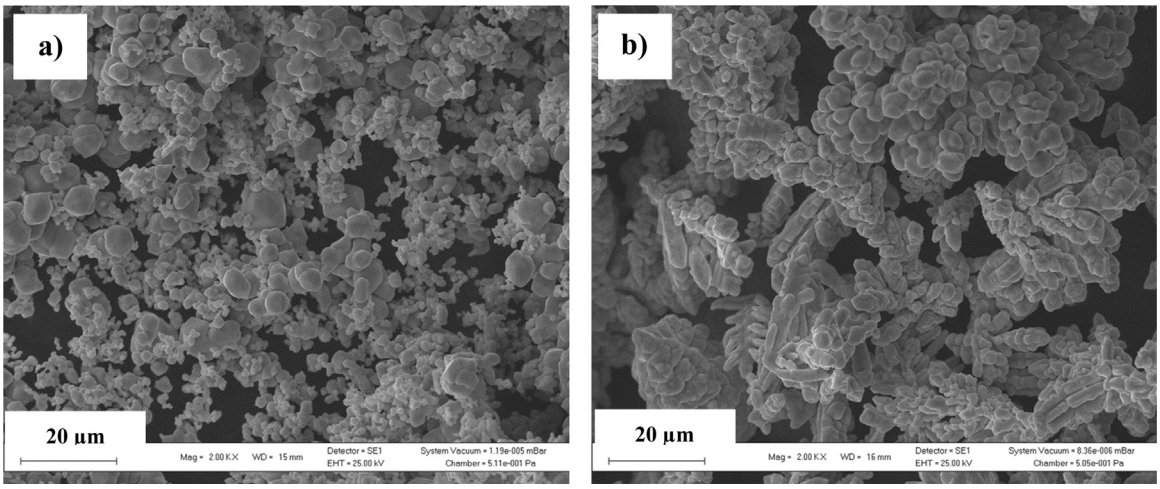

Fig. 1. SEM image of the (a) Mo and (b) Cu powders used in the study.

microhardness of sintered samples were measured using Struers micro-indentation machine with the load of 1960 mN for a dwelling time of 10 s. At least 5 indentations were made for each specimen.

3. Results

The morphology and size of the powders used as feedstock for this study are presented in Fig. 1. As it can be seen in Fig. 1a, a bimodal distribution of Mo powders containing agglomerated small particles with the size in the range of 1–4 µm and long with the larger irregular polyhedron powders with the size between 8 and 14 µm. Fig. 2b shows Cu irregular dendritic powders with sizes between 30 and 50 µm.

With the X-Ray Diffraction, the study of the progress of the changes in the crystallite size and the dislocation density of the MA powders, depending on the hours of milling, were undertaken. The samples analyzed by XRD were taken at 10, 20 and 30 h after the start of the process (see Fig. 2).

According to the values obtained with the XRD analysis, the average crystallite size and microstrain were obtained by the Williamson-Hall classic method for Mo and Cu [12]. The density of dislocations was calculated from the values of microstrain. The results are summarized in Table 2.

As can be seen in Table 2, there is strong microstructural refinement and strain hardening.

The decrease in the density of dislocations between 10 h and 20 h, may be attributed to a recovery or to the effects of a dynamic recrystallization due to the severe plastic deformation and a local increase in the temperature reached by the powders.

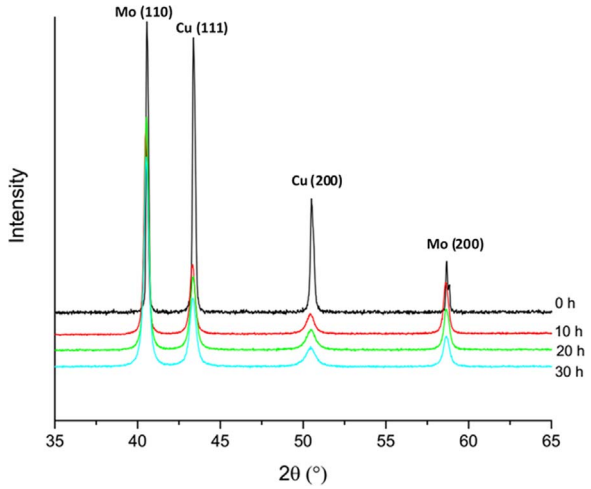

Fig. 2. X-ray diffraction of powder samples MA powders.

Table 2
Density of dislocations and average crystallite Mo and Cu size.

Milling time, h	Crystal size, nm	Mo Dislocation density, m^{-2}	Cu Dislocation density, m^{-2}
10	18	8.0E+17	4.6E+17
20	10	9.5E+17	7.1E+ 16
30	11	8.8E+17	3.7E+17

After the compaction stage, the green density of the samples was evaluated. Green densities of all types of samples compacted at 450 MPa are show in Fig. 3.

Fig. 4 shows the densities of compacted samples at 450 MPa after sintering at 1150 °C for 1 h.

Fig. 5 presents the porosity results (as the difference between theoretical density and sinter density) for the different types of sintered specimens.

Figs. 6–8 show the microstructure of sintered with compositions of Mo 10, 20, 30 vol% Cu formed by simple mixing, Mo + (Mo + Cu) m - Ar, Mo + (Mo + Cu) m - Ar + 10 vol% H_2 and MA powders.

Fig. 9 shows the Vicker's hardness of sintered specimens.

4. Discussion

4.1. Effects of % v Cu and milling on Mo-Cu powders sintered in Ar + 10 vol% H_2 for 30 h of grinding

4.1.1. Green density

Fig. 3 demonstrates green densities of samples which increase with increasing Cu content in the simple mix and MA powder composites without affecting density of Mo + (Mo + Cu) samples, which can be attributed to high ductility of copper powders allowing higher plastic deformation during compaction. The higher green densities obtained by simple mixing with values between 72% and 75% comparing with the higher green densities in the range of 63–68% obtained for MA powders confirm the effect of hardening by plastic deformation and decrease of green density.

4.1.2. Density after sintering

As can be seen in Fig. 4, sintered densities increase with increasing vol% Cu contents for samples because liquid Cu fills the pores and allows the union of the particles of Mo as a result of liquid propagation by capillary forces [5,13].

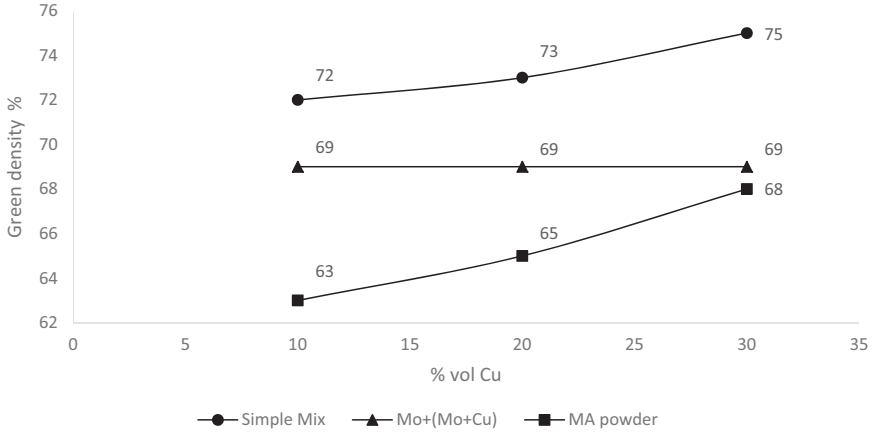

Fig. 3. Green density of compacted specimens at 450 MPa and 30 h of milling.

Among all samples, the MA samples reach the highest relative density 88% after sintering because the powders subjected to MA probably formed solid solutions of the Mo and Cu as reported by Suryanarayana [14]. This could be due to a homogeneous distribution of the Cu in the Mo, preventing the formation of Cu pools during the LPS and increasing the homogeneity of the microstructure as can be seen in Figs. 6c-7c and 8c for the different vol% Cu.

4.1.3. Microstructure

The microstructure of the samples of sintered MA powders is very fine and homogeneous with a laminar morphology of Cu and Mo as a result of the high energy grinding and little porosity, see Figs. 6, 7 and 8. The porosity, measured as the difference between theoretical and experimental density, results in $\varepsilon = 12–23\%$. The difference in porosity observed in micrographs and measured relative densities may be due to the metallographic polishing plastically deforming the surface of the sample and covering the pores.

On the other hand, the microstructure of simple mixed sintered samples are formed by a porous matrix of Mo, clear phase, considering it as nominal phase with higher vol% in the alloy, with Cu islands, which increase in size and quantity on the matrix, as it increases vol%, in this case it can be observed as the dark phase (see Figs. 7d and 8d). The low porosity reached, $\varepsilon = 24–27\%$ (Fig. 5) decreases as the vol% of Cu increases, which may be attributed to the fact that the liquid phase proportion in the sintering is spread between phase of Mo, and this improves densification.

4.1.4. Hardness

As can be seen in Fig. 9, the samples formed by MA powders showed the highest hardness reaching 182 HV without being affected by the vol % of Cu. This result indicates that, in the case of sintered MA powders, the high hardening may be caused by a fine dispersion of the Mo powders, it predominates over the amount of vol% Cu and the porosity over the hardness, as shown in Figs. 9–10.

The hardness of the other samples, on the other hand, decreases with the increase of vol% of Cu. In addition, for a given amount of Cu in the alloy, the hardness is inversely related to the porosity: as the porosity increases, the hardness decreases, as shown in Fig. 10.

For each samples, it can be seen how the porosity negatively affects the hardness, causing a lower resistance to the plastic deformation by indentation.

4.2. Effects of the addition of Mo elemental powders to mechanically alloyed Mo-Cu powders

4.2.1. Green density

The samples of Mo + (Mo + Cu) m have a green density value close to 69%, independent of % v Cu as can be seen in Fig. 4. Therefor, his approximately constant value of density could be determined by the constant amount of soft powders, in this case Mo, unmilled powders.

4.2.2. Microstructure

Comparing the samples made with mixtures of elemental powders of Mo and Cu, plus elemental powders of Mo, versus the sample with MA, clear differences in the microstructure obtained after sintering are observed, which can be observed in Figs. 6–8. The sample made with powders submitted to MA presents a homogeneous microstructure with a minimum presence of pores, which could be attributed to a homogeneous distribution of the Cu powders in the Mo matrix, and to a possible solids solution in MA of the Cu in the Mo. Unlike the other samples, where a marked delimitation between both phases, Cu and Mo is observed, due to the low immiscibility between them and a marked

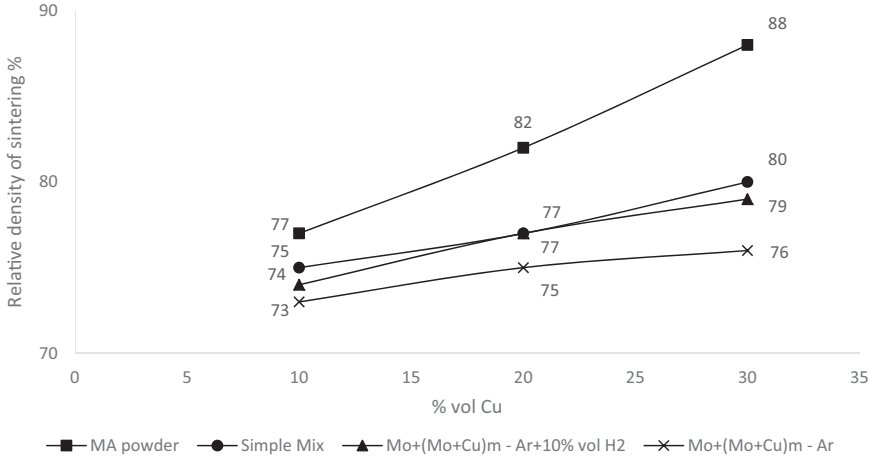

Fig. 4. Relative density of sintering at 1150 °C for 1 h with 30 h of milling.

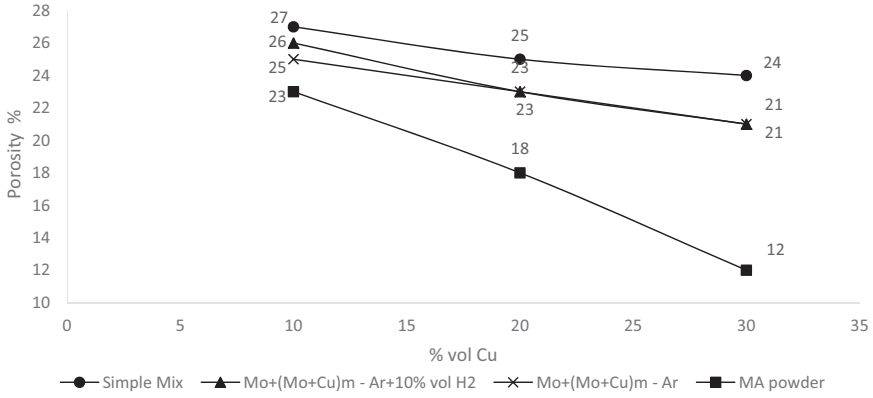

Fig. 5. Porosity graph of sintered specimens at 1150 °C for 1 h.

porosity in the samples.

4.3. Effects of the sintering atmosphere: Ar and Ar + 10 vol% H2, Mo + (Mo + Cu)m powders

The samples subjected to a reducing atmosphere (Ar + 10% H_2), possess densities higher than those exposed to neutral atmosphere Ar, which can be attributed to reduction of the surface oxide in Mo and Cu powders by H_2 and, thus, most likely improving wettability of the liquid Cu on the solid Mo [5]. Since the green density was the same for the sintered samples in both atmospheres, the densification follows the same trend as the density.

4.3.1. Microstructure

In general, the microstructure of the Mo + (Mo + Cu) m- (Ar + 10% H_2) samples shows a microstructure of Cu islands between larger and somewhat more oriented Mo islands than those sintered in the atmosphere (Ar-10 vol% H_2). The presence of a higher porosity and a larger grain size were also observed in the sintered samples in Ar. a porosity that decreases with increasing Cu content in the alloy.

4.3.2. Hardness

The hardness of the samples Mo + (Mo + Cu) m- (Ar + 10% H_2) is slightly higher than that of samples sintered in the atmosphere of Ar. It can be observed in Fig. 10 that the hardness depends not only on its porosity but also on the other factor that differentiates the samples is the size of each phase (Mo and Cu). The finer microstructure obtained in the sintering in Ar + 10 vol% H_2 (see micrographs a and b in Figs. 6, 7 and 8) has a higher hardness with similar porosity. That is to say, the difference of hardness between the samples sintered in Ar versus those sintered in (Ar + 10 vol% H_2), is not attributable only to the difference in porosity but also due to the microstructural refinement.

Fig. 10 shows the effect of porosity on hardness for each series of samples. For the same porosity, the MA sintered (Mo + Cu) m- (Ar +

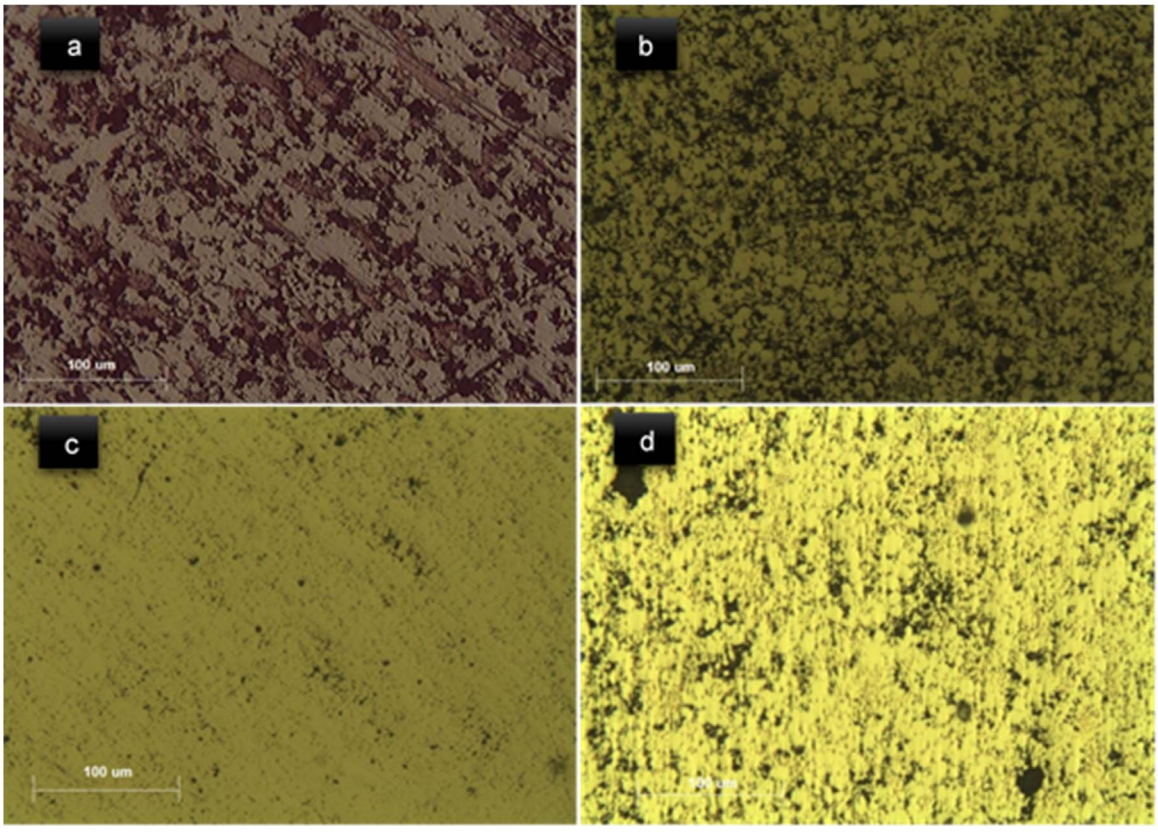

Fig. 6. Microstructure of Mo − 10 vol% Cu alloy sintered: a) Mo (Mo + Cu) m – Ar; b) Mo + (Mo + Cu) m - Ar + 10 vol% H_2; c) MA powders and d) Simple mixing. Optical microscopy. 30 h of milling.

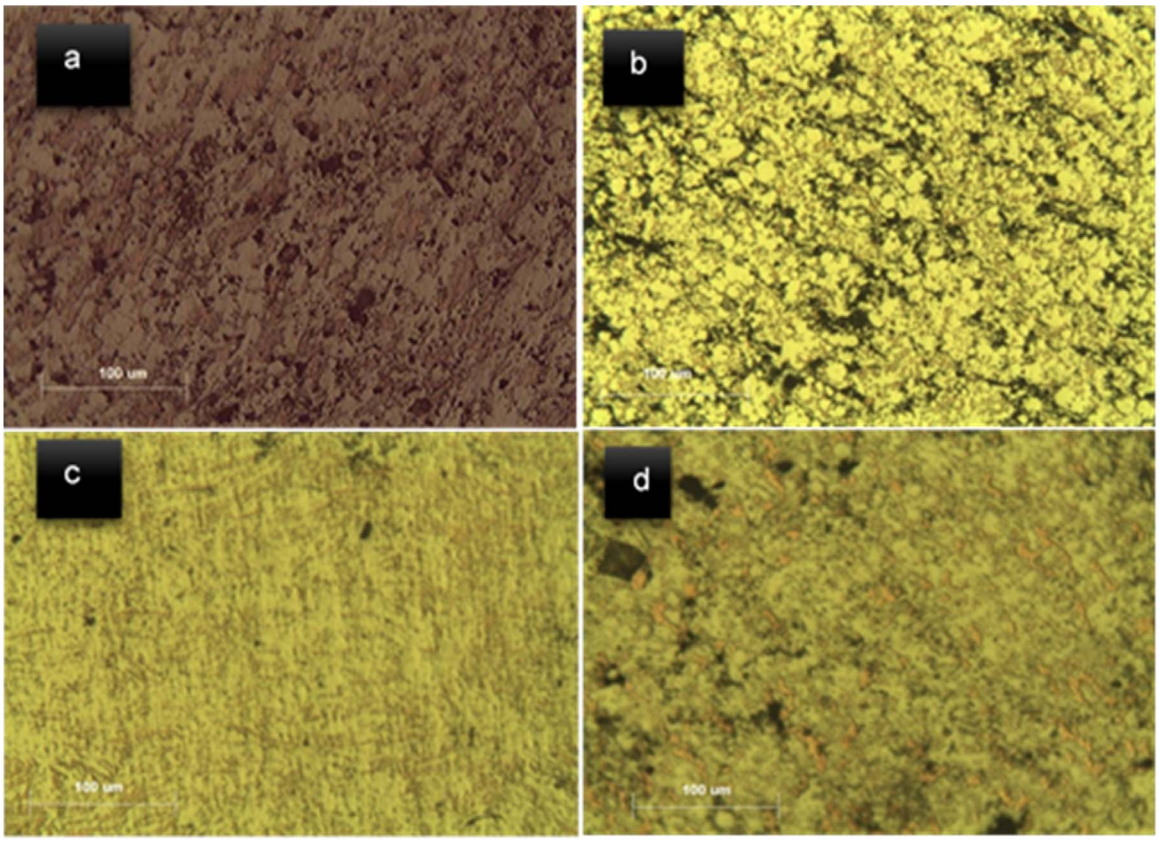

Fig. 7. Microstructure of Mo-20 vol%. Cu alloy sintered: a) Mo (Mo + Cu) m – Ar; b) Mo + (Mo + Cu) m - Ar + 10 vol% H_2; c) MA powders and d) Simple mixing. Optical microscopy. 30 h of milling.

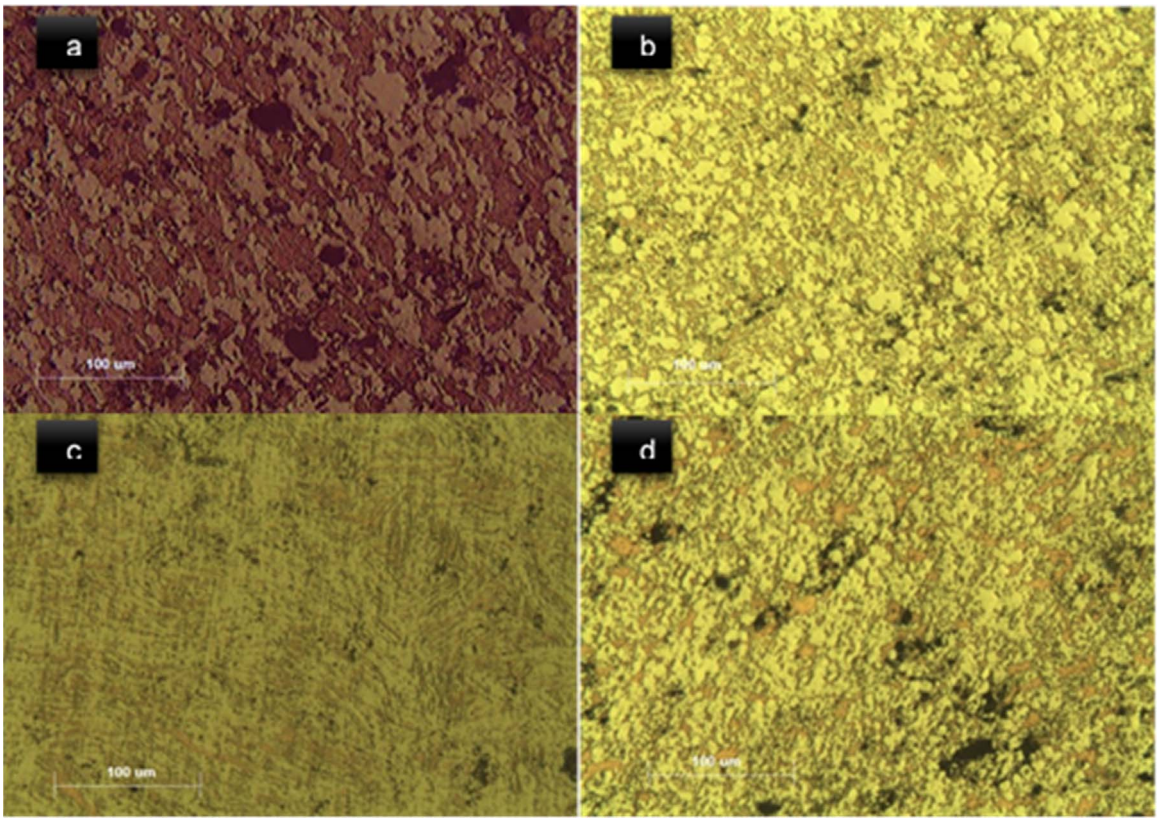

Fig. 8. Microstructure Mo-30 vol%. Cu alloy sintered: a) Mo (Mo + Cu) m - Ar, b) Mo + (Mo + Cu) m - Ar + 10% H2, c) MA powders and d) Simple mixing. Optical microscopy. 30 h of milling.

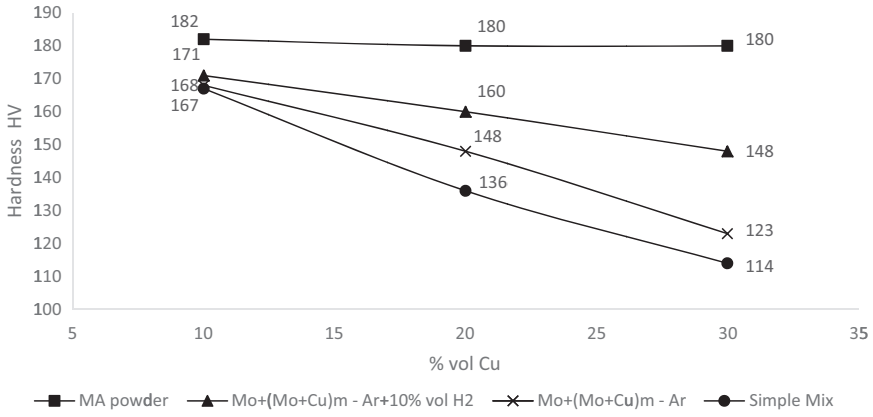

Fig. 9. Hardness vs vol% Cu in the sintered alloy, after 30 h of milling.

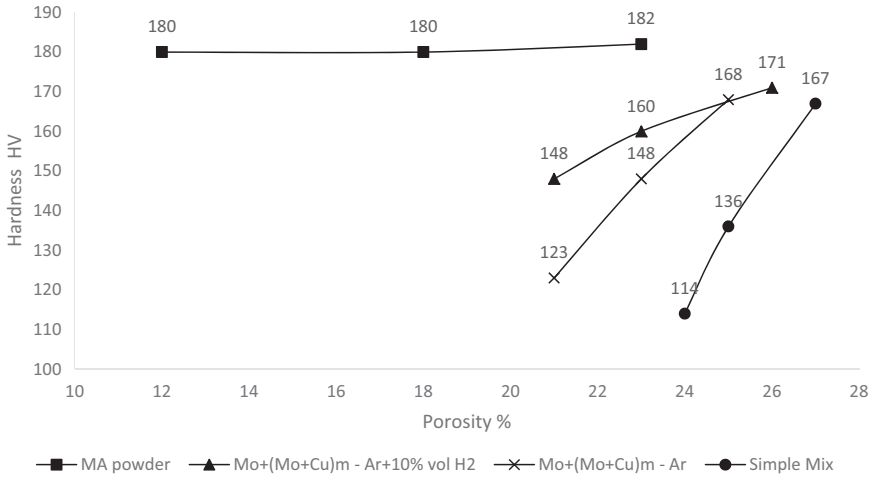

Fig. 10. Hardness vs % porosity in the sintered alloy, after 30 h of milling.

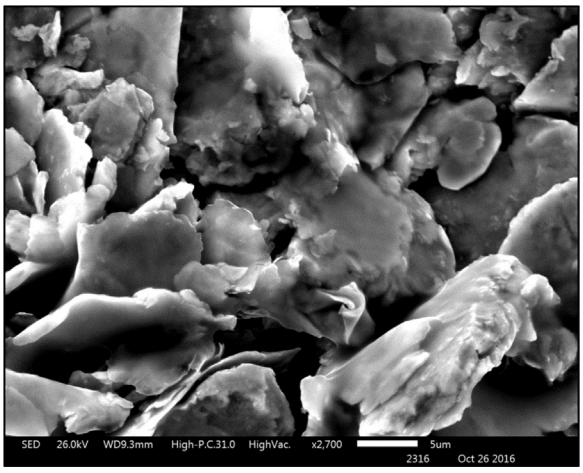

Fig. 11. Flakes produced after milling of Mo − 35 wt% Cu powders for 20 h of milling.

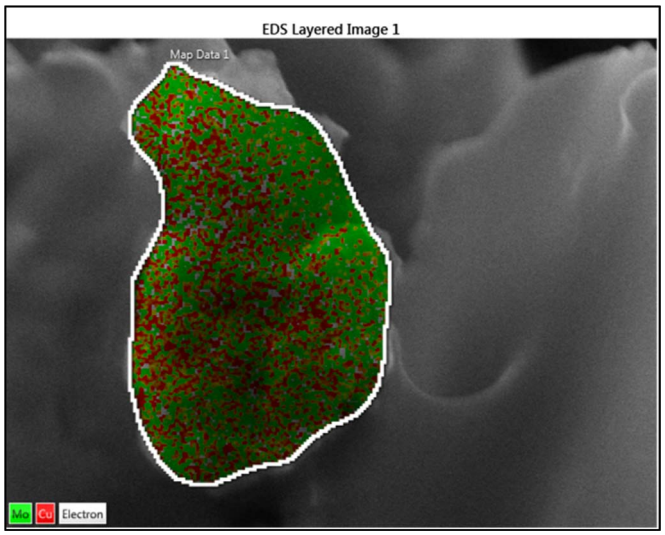

Fig. 12. Elemental analysis map showing the Mo and Cu distribution in a milled particle after 20 h of milling.

10 vol% H_2) samples showed the highest hardness and only mixed and sintered samples showed the lowest hardness, which can be attributed to the microstructural refinement and increase of dislocations density in the Mo powders, which occurs during the mechanical alloying. Both effects, deformation hardening and microstructural refinement in Mo powders, persist even after sintering at 1150 °C. It is known that the solid phase of molybdenum does not recrystallizes at this temperature. [15].

4.4. Solid solution Mo-Cu

In this work, it has been assumed that, during the mechanical alloying, Mo atoms enter into solid solution in the Cu powders. The results of XRD analysis (Fig. 2), show the existence of two phases: one phase rich in Mo and one phase rich in Cu. The data obtained for the diffraction angles and the relative intensities are not conclusive, when determining the incorporation of an element in the powders of the other element. For this reason, samples of Mo elemental powders were fabricated with 35 wt% Cu by mechanical alloy for 20 h, then sintered for one hour at 1150 °C in Ar atmosphere, and analyzed by EDS and SEM.

In the SEM image in Fig. 11, the flake morphology of the powders is

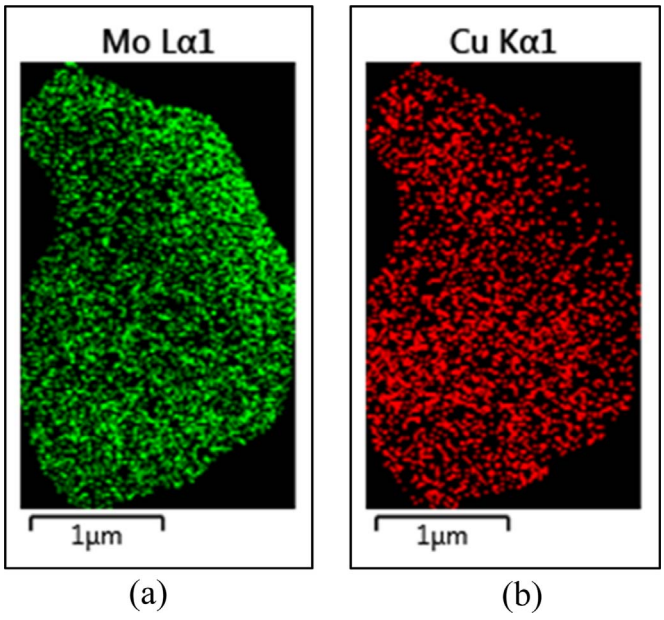

Fig. 13. Mapping of the (a) Mo and (b) Cu distribution in the Mo-35 wt% Cu powder particle. 20 h of MA.

shown. The elemental analysis and mapping by EDS (Figs. 12 and 13) evidence homogeneous distribution of both Mo and Cu in the particle, which indicates that a solid solution of Mo and Cu is formed or a strong reduction of the size of the Mo and Cu particles occurred at nanometric levels.

5. Conclusions

MA and sintered powders have the highest sintered densities of all studied alloys, which can be explained by the formation of solid solution of Mo in Cu during MA, evidenced by the EDS analysis. It is suggested, that sample reach the highest hardness due to their microstructural refinement, high density of Mo and Cu dislocations and low porosity.

The increase of Cu in the samples increases the density and interconnection, which is due to the increase of the liquid phase in sintering through the increase of the amount of Cu in the alloy.

Adding unmilled Mo to the powder mixture (Mo + Cu)m effectively increases the green density comparing with 100% milled Mo-Cu powders; however, its densification is not high enough so that the density after sintering is greater than that of the milled and sintered powders.

The use of a reducing atmosphere (Ar + 10 vol% H_2) has a positive effect on densification and density due to its ability to remove surface oxides from Mo and Cu powders. The samples formed with powders alloyed with Mo showed an average improvement of 2.3% in the sintering density and 7.4% in the densification, in relation to the same sintered powders in only Ar.

Acknowledgement

The authors thank Molibdenos y Metales SA, Molymet, for supplying Mo powders and facilitate the equipment for sintering and analyzing the samples using SEM. P. Benavides is grateful for the funding of his Ph.D. studies awarded by the Universidad Tecnológica de Chile INACAP and the Faculty of Physical and Mathematical Sciences of the University of Chile.

References

[1] G. Jiang, L. Diao, K. Kuang, Adv. Therm. Manag. Mater. (2013) 164, http://dx.doi.org/10.1007/978-1-4614-1963-1.
[2] J.-T. Yao, C.-J. Li, Y. Li, B. Chen, H.-B. Huo, Relationships between the properties and microstructure of Mo–Cu composites prepared by infiltrating copper into flame-sprayed porous Mo skeleton, Mater. Des. 88 (2015) 774–780, http://dx.doi.org/10.1016/j.matdes.2015.09.062.
[3] C. Guo-qin, J. Long-tao, W.U. Gao-hui, Fabrication and characterization of high dense Mo / Cu composites for electronic packaging applications, 2007.
[4] J. Liu, R.M. German, Rearrangement densification in liquid-phase sintering, Metall. Mater. Trans. A. 32 (2001) 3125–3131, http://dx.doi.org/10.1007/s11661-001-0187-6.
[5] R.M. German, P. Suri, S.J. Park, Review: liquid phase sintering, J. Mater. Sci. 44 (2009) 1–39, http://dx.doi.org/10.1007/s10853-008-3008-0.
[6] M.S. El-Eskandarany, The history and necessity of mechanical alloying, in: Mech. Alloy. Nanotechnology, Mater. Sci. Powder Metall., 2015, pp. 13–47. http://dx.doi.org/10.1016/B978-1-4557-7752-5.00002-4.
[7] V. de, P. Martínez, C. Aguilar, J. Marín, S. Ordoñez, F. Castro, Mechanical alloying of Cu-Mo powder mixtures and thermodynamic study of solubility, Mater. Lett. 61 (2007) 929–933, http://dx.doi.org/10.1016/j.matlet.2006.11.070.
[8] C. Aguilar, S. Ordoñez, J. Marín, F. Castro, V. Martínez, Study and methods of analysis of mechanically alloyed Cu-Mo powders, Mater. Sci. Eng. A 464 (2007) 288–294, http://dx.doi.org/10.1016/j.msea.2007.02.017.
[9] S. Xi, K. Zuo, X. Li, G. Ran, J. Zhou, Study on the solid solubility extension of Mo in Cu by mechanical alloying Cu with amorphous Cr(Mo), Acta Mater. 56 (2008) 6050–6060, http://dx.doi.org/10.1016/j.actamat.2008.08.013.
[10] F. Jinglian, C. Yubo, L. Tao, T. Jiamin, Sintering behavior of nanocrystalline Mo-Cu composite powders, Rare Met. Mater. Eng. 38 (2009) 1693–1697, http://dx.doi.org/10.1016/S1875-5372(10)60051-3.
[11] P. Song, J. Cheng, L. Wan, J. Zhao, Y. Wang, Y. Cai, Preparation and characterization of Mo-15 Cu superfine powders by a gelatification-reduction process, J. Alloy. Compd. 476 (2009) 226–230, http://dx.doi.org/10.1016/j.jallcom.2008.09.097.
[12] C. Aguilar, Análisis del tamaño de cristalita en aleaciones Cu-Mo procesadas por aleado mecánico, Rev. La Fac. Ing. 23 (2009) 1–8.
[13] N. Eustathopoulos, Wetting by liquid metals—application in materials processing: the contribution of the Grenoble Group, Metals (Basel) 5 (2015) 350–370, http://dx.doi.org/10.3390/met5010350.
[14] C. Suryanarayana, Mechanical alloying and milling, Prog. Mater. Sci. 46 (2004) 1–184, http://dx.doi.org/10.1016/S0079-6425(99)00010-9.
[15] S. Primig, H. Leitner, H. Clemens, A. Lorich, W. Knabl, R. Stickler, On the recrystallization behavior of technically pure molybdenum, Int. J. Refract. Met. Hard Mater. 28 (2010) 703–708, http://dx.doi.org/10.1016/j.ijrmhm.2010.03.006.